The Journal of Physical Chemistry A

 VOLUME 103, NUMBER 1, JANUARY 7, 1999

ARTICLES

Dielectric Relaxation of Aqueous NaCl Solutions

Richard Buchner,*,† Glenn T. Hefter,* and Peter M. May

Chemistry Department, Division of Science, Murdoch University, Murdoch, W.A. 6150, Australia

Received: July 10, 1998; In Final Form: October 14, 1998

The complex dielectric permittivity of aqueous sodium chloride solutions has been determined in the frequency range $0.2 \leq \nu(\mathrm{GHz}) \leq 20$ with a commercial dielectric measurement system based on a vector network analyzer. NaCl solutions $0.1 \leq m\ (\mathrm{mol\ kg^{-1}}) \leq 5$ (mass fraction $0.005 \leq w \leq 0.23$) were investigated at 5, 20, 25, and 35 °C. An improved calibration procedure of the dielectric measurement system for conducting samples was developed. The complex permittivity spectra have been represented by a Cole−Cole relaxation time distribution. Where possible, the obtained fitting parameters, static permittivity ϵ and relaxation time τ, and distribution parameter α, are compared with literature data to assess the performance of the instrument, which was found to be comparable to that of time domain and waveguide systems. Effective solvation numbers were deduced from the effect of NaCl concentration on ϵ. The data suggest that in addition to the irrotational bonding of water molecules by Na^+ ions, kinetic depolarization under *slip* boundary conditions determines the solution permittivity. A three-state model is proposed to describe the concentration dependence of τ.

1. Introduction

The dielectric relaxation behavior of electrolyte solutions yields important information on ion solvation and complexation, as well as on the impact of long-range ion−solvent interactions on the cooperative solvent dynamics, especially for hydrogen-bonding liquids.[1−6] The dielectric properties of solutions have important effects on charge transport,[7,8] chemical speciation,[1,9] and various thermodynamic properties of solutions.[10] Dielectric relaxation spectroscopy (DRS) also appears to be a promising tool for the investigation of weak ion-pair complexes,[11,12] which are important for understanding the properties of seawater,[13] geological brines,[14] and hydrometallurgical or other industrial electrolyte solutions.[15] An increasing need for dielectric data, characterizing the interaction of materials with microwaves, also arises from emerging technical applications, suchas dielectric heating,[16,17] moisture sensors,[18,19] and process control.[20]

However, despite their obvious importance, the available dielectric data even for aqueous solutions are rather limited and not always reliable.[21] A major reason for this is the technical difficulty associated with the determination of the complex (dielectric) permittivity spectrum of electrolyte solutions

$$\hat{\epsilon}(\nu) = \epsilon'(\nu) - \mathrm{i}\epsilon''(\nu) \qquad (1)$$

$\hat{\epsilon}(\nu)$ is a measure of the amplitude and the time dependence of the fluctuations of the total dipole moment of the sample, $\vec{M}(t) = \sum\vec{\mu}_j$, arising from the individual permanent molecular dipoles, $\vec{\mu}_j$, and the molecular polarizabilities, α_j. The dielectric dispersion curve, $\epsilon'(\nu)$ (where the static permittivity $\epsilon = \lim_{\nu\to 0}\epsilon'(\nu)$), indicates how far $\vec{M}(t)$ is able to keep pace with an external electric field of frequency ν, and the connected dissipation of electromagnetic energy is expressed by the dielectric loss, $\epsilon''(\nu)$.[22] For electrolyte solutions around ambient temperature, the frequencies for dielectric relaxation are in the microwave region, which requires special instrumentation. Access to this spectral range has become easier now with the commercial availability

* To whom correspondence should be adressed.

† Permanent adress: Institut für Physikalische und Theoretische Chemie, Universität Regensburg, D-93040 Regensburg, Germany. E-mail: Richard.Buchner@chemie.uni-regensburg.de.

10.1021/jp982977k CCC: $18.00
Published on Web 12/17/1998

of dielectric measurement systems based on vector network analyzers (VNAs). However, the reliable determination of the dielectric loss is a major challenge due to the high specific electric conductivity, κ, exhibited by many (and especially aqueous) electrolytes, because only the total loss of the sample

$$\eta''(\nu) = \epsilon''(\nu) + \eta''_\kappa = \epsilon''(\nu) + \kappa/(2\pi\nu\epsilon_0) \qquad (2)$$

is experimentally accessible;[22] ϵ_0 is the permittivity of the vacuum. Obviously, the Ohmic loss, η''_κ, swamps ϵ'' below a minimum frequency, ν_{min}, fixed by κ and the precision of the instrument, thus limiting the spectral range accessible to experiments.

Recently, Nörtemann et al. determined precise complex permittivity spectra of dilute ($w \leq 0.035$) aqueous NaCl solutions at 20 °C.[23] These data have been used to assess the performance of our VNA-based dielectric measurement system and to extend the measurements to molalities $m \leq 5$ mol kg^{-1} ($w \leq 0.23$) close to the saturation limit and temperatures $5 \leq \vartheta$ (°C) ≤ 35. The spectra have been fitted with a Cole−Cole relaxation time distribution. The resulting parameters are compared with the sparse literature data and discussed in terms of ionic solvation and solvent dynamics. Figure 1.

2. Experiment and Data Analysis

Dielectric experiments were performed with a Hewlett-Packard model HP 85070M Dielectric Probe System, consisting of a HP 8720D vector network analyzer (nominal bandwidth 50 MHz to 20 GHz) and a HP 85070 dielectric probe kit (200 MHz to 20 GHz recommended bandwidth). The HP 85070 dielectric software was used for controlling the instrument and for calculation of the dielectric permittivity, $\epsilon'(\nu)$ and total loss, $\eta''(\nu) = \epsilon''(\nu) + \eta''_\kappa(\nu)$, from the experimentally determined relative complex reflection coefficient of the probehead/sample interface at the frequency ν.

The probehead is mounted in a specially constructed stainless steel cell top that can be hermetically sealed to a glass cell body (30 mL sample volume) with a thermostating jacket. The cell top has stainless steel cannulas that allow the cell to be flushed with dry nitrogen during filling and dielectric measurement. Temperature control is achieved by an external thermostat (Julabo F33-SD, with an operating range − 30 to 200 °C controlled to ±0.01 °C) to an accuracy of ±0.1 °C or better, depending on the difference against ambient temperature.

Samples of 100 mL were prepared by weight from analytical grade NaCl (Ajax Chemicals, Australia) and Millipore (Milli-Q system) water. The density data required to convert solution molalities, m, to molar concentrations, c, as well as the specific conductivity, κ, necessary to calculate $\epsilon''(\nu)$ from $\eta''(\nu)$ were interpolated from appropriate fits to selected literature data provided by the ELDAR database.[26]

Dielectric experiments were performed for solution molalities in the range 0.1−5 mol kg^{-1} at 20 °C, where the recent investigation of Nörtemann et al.[23] allows the assessment of our instrumentation, as well as at 5, 25, and 35 °C. Excessive conductivity at the highest temperature prevented investigations above 4 mol kg^{-1}. For each series of measurements, usually comprising four to six samples, the VNA was calibrated with three standards, air, a short circuit, and Millipore water, thermostated to the desired measurement temperature. Each solution was measured at least twice in different measurement series and $\epsilon'(\nu)$ and $\eta''(\nu)$ were generally recorded at 101 frequencies equidistant on a logarithmic scale between ν_{min} and

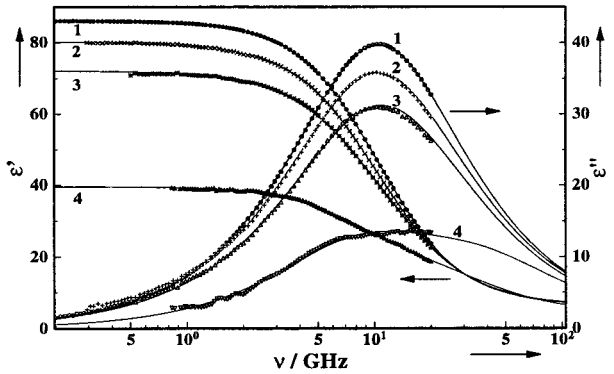

Figure 1. Dielectric dispersion, $\epsilon'(\nu)$, and loss spectrum, $\epsilon''(\nu)$, of NaCl solutions in water at 5 °C: spectrum 1, pure water; spectrum 2, $c = 0.400$ mol dm^{-3}; spectrum 3, $c = 0.990$ mol dm^{-3}; spectrum 4, $c = 4.643$ mol dm^{-3}. Experimental spectra 1−3 (symbols) are fitted to a single Cole−Cole equation (lines); spectrum 4 is fitted to a superposition of two Debye processes.

$\nu_{max} = 20.05$ GHz. The value of $\nu_{min} \geq 0.2$ GHz was adapted to the conductivity of the sample; see Figure 1.

In the frequency window of the VNA, $0.05 \leq \nu$(GHz) ≤ 20.05, the dielectric spectrum of the calibration standard water can be modeled by a Debye equation. The static permittivity, $\epsilon(\vartheta)$, was interpolated with the help of the equation

$$\epsilon(\vartheta) = 87.85306 \exp(-0.00456992\vartheta); \quad -35 \leq \vartheta\ (°C) \leq 100 \qquad (3)$$

derived by Ellison et al. from a comprehensive survey of available literature data.[25] The relaxation time, $\tau(\vartheta)$, and the high-frequency permittivity, $\epsilon_\infty(\vartheta)$, were obtained as smoothed parameters for the primary (low-frequency) relaxation process of water obtained by fitting a superposition of two Debye processes (2D model) to the experimental $\hat{\epsilon}(\nu)$ data of refs 21, 25, and 27−29. In the temperature range $0 \leq \vartheta$ (°C) ≤ 55, the parameters $\tau(\vartheta)$ and $\epsilon_\infty(\vartheta)$ can be interpolated with the equations

$$\frac{\tau(\vartheta)^{-1}}{\text{ps}} = (5.631 \pm 0.015) \times 10^{-2} + (2.12 \pm 0.03) \times 10^{-3}\frac{\vartheta}{°C} + (1.86 \pm 0.09) \times 10^{-5}\left(\frac{\vartheta}{°C}\right)^2 \qquad (4)$$

and

$$\epsilon_\infty(\vartheta) = (6.49 \pm 0.08) - (0.025 \pm 0.002)\frac{\vartheta}{°C} \qquad (5)$$

The above parameters for the 2D model give an optimum description of the water band shape in the frequency range of the VNA. However, it should be noted that the same data yield comparable relaxation times and only a minor shift of the "infinite frequency permittivity", $\epsilon_\infty^{1D}(\vartheta) = \epsilon_\infty^{2D}(\vartheta) - 0.22$, if a single Debye process (1D model) is fitted to $\hat{\epsilon}(\nu)$ at $\nu \leq 40$ GHz.

The first series of experiments at 20 °C, performed with the shorting block provided with the HP 85070 dielectric probe kit as the short circuit standard, showed that the accuracy and the reproducibility of the instrument (although well within the specifications of the manufacturer) had to be improved for the investigation of highly conducting samples. It was found that the electrical contact of the probehead and the block was not sufficiently reproducible to reach the 2.5% error limits required for the unambiguous separation of $\epsilon''(\nu)$ from $\eta''(\nu)$. A comparative investigation with the shorting block and mercury

as the short circuit standards revealed better overall performance and higher reproducibility for the latter. Mercury was thus used in all subsequent experiments.

After correction of the total loss of the sample, $\eta''(\nu)$, for the conductivity contribution, $\eta''_\kappa(\nu) = \kappa/(2\pi\nu\epsilon_0)$, the real, $\epsilon'(\nu)$, and imaginary, $\epsilon''(\nu)$, parts of the complex permittivity spectrum were fitted simultaneously to a relaxation model of the type

$$\hat{\epsilon}(\nu) = \sum_{j=1}^{n} S_j \tilde{F}_j(\nu) + \epsilon_\infty \tag{6}$$

where $S_j = \epsilon_j - \epsilon_{j\infty}$ is the amplitude of the individual relaxation process j from a superposition of n dispersion steps and the "static" permittivity of the solution is defined as

$$\epsilon = \lim_{\nu \to 0} \epsilon'(\nu) = \sum_{j=1}^{n} S_j + \epsilon_\infty$$

In the time scale of the experiment, the molecular polarizability is always in equilibrium with the external field and can be summarized in the "infinite frequency" permittivity ϵ_∞. The relaxation functions $\tilde{F}_j(\nu)$ of the individual dispersion steps were represented as Havriliak−Negami equations

$$\tilde{F}_j(\nu) = [1 + (i2\pi\nu\tau_j)^{1-\alpha_j}]^{-\beta_j} \tag{7}$$

or, as the special cases thereof, the Cole−Davidson relaxation time distribution with $0 < \beta_j \leq 1$ and $\alpha_j = 0$, the Cole−Cole equation with $\beta_j = 1$ and $0 \leq \alpha_j < 1$, or the Debye relaxation process with $\alpha_j = 0$ and $\beta_j = 1$; τ_j is the relaxation time of process j.[22] Software based on the Gauss−Marquardt algorithm was used to optimize the goodness of the fit and to obtain the variances, s^2, for comparison of the different relaxation models.[31]

Several plausible relaxation models were tested. In all cases, it transpired that κ had to be treated as an adjustable parameter giving values between 93% and 110% of the ELDAR data summarized in Tables 3S−6S of the Supporting Information. This "effective" conductivity depends on the concentration and on the temperature of the sample but is reproducible within 2% and independent of the relaxation model. It seems likely that the mathematical model for the probehead/sample interface implemented in the HP 85070 dielectric software is inadequate at high conductivities for the reasons discussed in ref 24.

All the spectra could be fitted with a single Cole−Cole equation. At all temperatures, ν_{max} is comparable to $(2\pi\tau)^{-1}$. Therefore, the extrapolation of $\epsilon'(\nu)$ to the infinite frequency permittivity is very sensitive to experimental errors. The upper frequency limit of 20 GHz also prevents the separation of the small high-frequency relaxation process ($\tau_2 \approx 1$ ps) reported for pure water.[27,28,30] It was observed that the electrolyte results obtained for ϵ_∞ scatter around the value of pure water if this quantity is treated as an adjustable parameter in the fitting procedure. Additionally, the values of τ and α are comparable to the data given below, but the variance of the fit is generally increased. Therefore, ϵ_∞ was preset in all fits of the electrolyte spectra yielding the parameters ϵ, Figure 2, τ, Figure 3, and α, Figure 4, summarized in Tables 3S−6S of the Supporting Information. At 5 and 25 °C, the 1D model results of pure water, $\epsilon_\infty(5\ °C) = 6.14$ and $\epsilon_\infty(25\ °C) = 5.65$ were used, whereas at 35 °C the value of eq 5, $\epsilon_\infty(35\ °C) = 5.60$, was preferred since the dielectric loss peak lies outside the accessible frequency window. However, it should be noted that the changes of ϵ, τ, and α produced by setting $\epsilon_\infty(35\ °C) = \epsilon_\infty{}^{1D}$ are at least a factor of 10 smaller than the scatter of these parameters between different measurement series (calibrations). To allow a direct comparison with the data of ref 23, their value of $\epsilon_\infty(20\ °C) = 5.6$ was used.

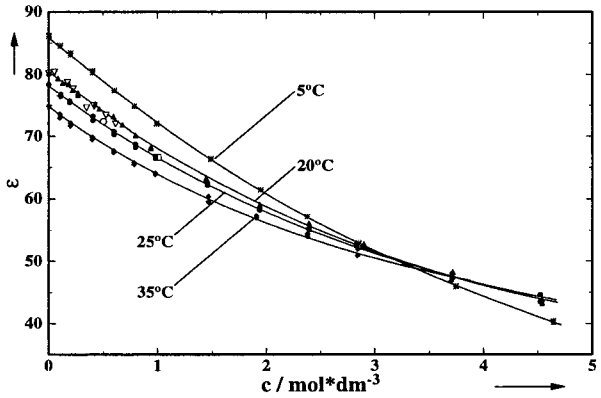

Figure 2. Experimental data (closed symbols) and fitted polynomials, eq 8, of the solution permittivity, ϵ, of NaCl solutions in water as a function of electrolyte concentration and temperature. Literature data for ϵ are as follows: refs 32 (+), 33 (○), and 34 (□) at 25 °C, and ref 23 (▽) at 20 °C.

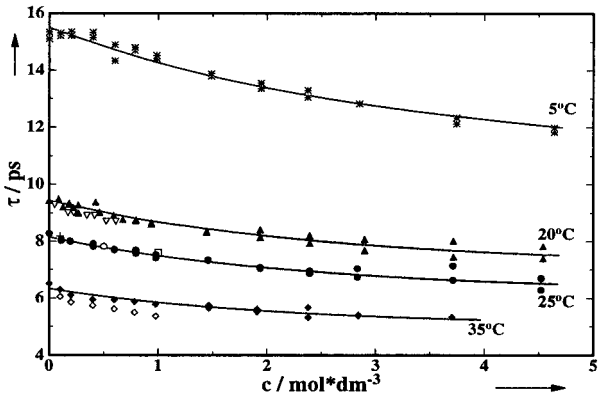

Figure 3. Experimental data (closed symbols) and fits of the three-state model (eq 21) of the solvent relaxation time, τ, of NaCl solutions in water as a function of electrolyte concentration and temperature (data with open symbols at 35 °C not included in the fit). Literature data for τ are as follows: refs 32 (+), 33 (○), and 34 (□) at 25 °C, and ref 23 (▽) at 20 °C.

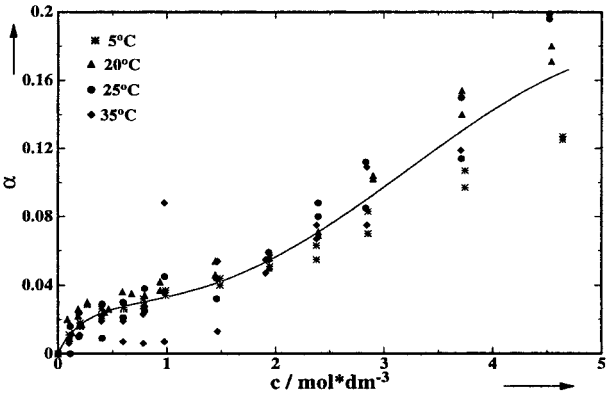

Figure 4. Experimental Cole−Cole relaxation time distribution parameters, α, of NaCl solutions in water as a function of electrolyte concentration and temperature: (∗) 5 °C; (▲) 20 °C; (●) 25 °C; (◆) 35 °C. The line represents the best fit of the polynomial $\alpha(c) = \sum a_i c^{1/2}$, $i = 2-5$, to the entire data set.

Although a reasonable fit to the experimental spectra was achieved using the Cole−Cole equation, it should be noted that the variance, s^2, increases with concentration (see column 11

TABLE 1: Coefficients $y(0)$, δ, and β of the Polynomial (8), Valid up to c_{max}, for the Solution Permittivity $\epsilon(c)$ and for the Relaxation Time $\tau(c)$ of Aqueous NaCl Solutions as a Function of Temperature, ϑ, Standard Errors of the Fits, $\sigma_{fit}(\epsilon)$ and $\sigma_{fit}(\tau)$, Static Permittivity of Water, ϵ_{lit}, According to Ref 25, and Water Relaxation Time of eq 4, τ_{cal}[a]

ϑ	ϵ_{lit}	$\epsilon(0)$	δ_ϵ	β_ϵ	$\sigma_{fit}(\epsilon)$	c_{max}
5	85.87	86.46 ± 0.07	18.18 ± 0.14	3.81 ± 0.07	0.18	4.65
		86.11 ± 0.06	14.29 ± 0.11		0.15	1.0
20	80.18	80.73 ± 0.18	16.8 ± 0.4	4.1 ± 0.2	0.45	4.55
		80.42 ± 0.11	12.7 ± 0.3		0.24	0.8
25	78.37	78.14 ± 0.13	15.2 ± 0.3	3.64 ± 0.13	0.30	4.53
		78.12 ± 0.16	12.8 ± 0.4		0.27	0.6
35	74.87	74.42 ± 0.18	13.9 ± 0.5	3.4 ± 0.2	0.37	3.70
ϑ	τ_{cal}	$\tau(0)$	δ_τ	β_τ	$\sigma_{fit}(\tau)$	c_{max}
5	14.84	15.36 ± 0.08	1.2 ± 0.2	0.21 ± 0.08	0.22	4.65
20	9.42	9.41± 0.06	1.10 ± 0.13	0.33 ± 0.06	0.15	4.55
25	8.27	8.15 ± 0.06	0.91 ± 0.12	0.27 ± 0.06	0.14	4.53
35	6.52	6.34 ± 0.06	0.81 ± 0.14	0.29 ± 0.08	0.13	3.70

[a] Units: ϑ in °C, δ_ϵ in dm^{-3} mol^{-1}. β_ϵ in dm$^{-9/2}$ mol$^{-3/2}$. c_{max} in mol dm^{-3}. τ_{cal}, $\tau(0)$, and $\sigma_{fit}(\tau)$ in 10^{-12} s; δ_ϵ in 10^{-12} s dm^{-3} mol^{-1}; β_τ in 10^{-12} s dm$^{-9/2}$ mol$^{-3/2}$.

of Tables 3S−6S) of the Supporting Information. This is due in part to the appearance of oscillations on the spectra (Figure 1), which suggest calibration inadequacies due to the large difference between the dielectric properties of the sample and those of water. Nevertheless, the increasing deviation of the overall band shape from a Cole−Cole relaxation time distribution at high concentrations appears to genuinely reflect the relaxation behavior of the solutions. At 5 °C and $m \geq 1$ mol kg^{-1}, the superposition of two Debye processes achieves a considerably better fit; that is, s^2 improves by a factor of 2−3 with reasonable relaxation parameters (Table 7S of the Supporting Information). Although this observation should not be overinterpreted, since the high-frequency process is centered outside the accessible frequency window, it supports the three-state model suggested in the discussion of the relaxation times below.

3. Results

The permittivity of the solutions, $\epsilon(c)$, at each temperature can be adequately fitted over the entire concentration range of the experiments by the polynomial

$$y(c) = y(0) - \delta c + \beta c^{3/2}; \quad y = \epsilon, \tau \tag{8}$$

with the parameters collected in Table 1. However, it should be noted that, at 5 and 20 °C (and also at 25 °C albeit to a lesser extent), $\epsilon(c)$ decreases linearily up to fairly high concentrations. It is therefore better to set $\beta_\epsilon = 0$ for fitting $\epsilon(c)$ at low c. The resulting parameters are also given in Table 1. Experimental data and fits are compared in Figure 2. In all cases, the maximum deviation of $\epsilon(c)$ from the fit curve is less than 2%. As can be seen from a comparison of the parameter $\epsilon(0)$ in Table 1 with the permittivity of pure water given by Ellison et al.,[25] our data do not support the ion atmosphere polarization effects[8] discussed by Nörtemann et al. at low concentrations.[23] Interestingly, however, the data indicate a crossover in the temperature depence of $\epsilon(c)$ around 3.5 mol dm^{-3} (Figure 2).

For all temperatures investigated, the relaxation times, $\tau(c)$, decrease monotonically with increasing electrolyte concentration (Figure 3). The data can be described either by eq 8, cf. Table 1, or by the three-state model suggested in Section 4.2. The intercept, $\tau(0)$, is larger at 5 °C and smaller at 25 and 35 °C compared to the calibration value of eq 4. Together with the measurement series represented in Figure 3 by the open symbols at 35 °C, which reveals some problem with instrument calibration, this may indicate systematic shifts in $\tau(c)$. However, the smooth and gentle concentration dependence of the Arrhenius activation energy $E_a(\tau)$ does not favor such an interpretation; data indicate a maximum, $E_a = 21.7 \pm 0.7$ kJ mol^{-1}, around 0.8 mol dm^{-3} compared to $E_a = 19.6 \pm 0.4$ kJ mol^{-1} for pure water and 19.7 ± 0.5 kJ mol^{-1} at $c = 4.5$ mol dm^{-3}.

As a result of the limited accessible frequency range, the Cole−Cole relaxation time distribution parameters, α, show considerable scatter (Figure 4). Nevertheless, the data indicate that over the temperature range investigated the spectra are close to Debye behavior up to approximately 1.5 mol dm^{-3}. At higher concentrations, α increases significantly and, eventually, a trend with temperature becomes apparent.

Literature data can be used to assess the accuracy of the VNA. Figure 2 shows that our $\epsilon(c)$ at 20 °C agree well with the recent data of Nörtemann et al.[23] but show less scatter. At 25 °C, our results agree nicely with the data of refs 32−34. Similar agreement with the quoted publications is observed for τ (Figure 3). Our results for δ_ϵ are in good agreement with the initial slopes of Nörtemann et al.[23] ($\delta_\epsilon = 13.6$ dm^3 mol^{-1}), Hasted[35] (11.2 dm^3 mol^{-1}), Zasetskii et al.[36] (15.2 dm^3 mol^{-1}), and Strogyn[37] (16.8 dm^3 mol^{-1}) at 20 °C, as well as the data of Kaatze[33] (11.2 dm^3 mol^{-1}) at 25 °C. From δ_τ, a relative molar shift of the solvent relaxation time may be calculated according to

$$B_c = \frac{1}{\tau} \lim_{c \to 0} \left(\frac{d\tau}{dc}\right) = \frac{\delta_\tau}{\tau} \tag{9}$$

Using the data of Table 1, the values B_c(5 °C) = −0.080 ± 0.011 dm^3 mol^{-1}, B_c(20 °C) = −0.117 ± 0.014 dm^3 mol^{-1}, B_c(25 °C) = −0.112 ± 0.014 dm^3 mol^{-1}, and B_c(35 °C) = −0.17 ± 0.02 dm^3 mol^{-1} were obtained. When the small difference between molarity and molality for dilute aqueous solutions is neglected, these data compare well with the molal shifts given by Nörtemann et al.,[23] B_d(20 °C) = −0.15 ± 0.06 kg mol^{-1} and B_d(25 °C) = −0.08 ± 0.03 kg mol^{-1}. This suggests that around room temperature at $c \leq 1$ mol dm^{-3} we can determine the static permittivity within about ±1%, whereas an accuracy on the order of ±0.2 ps is estimated for τ.

At higher concentrations and at other temperatures, only limited data are available for comparison. Since the scatter of these data is very large, they are not included in the graphs for clarity. At 25 °C the $\epsilon(c)$ values of Barthel et al.[38] are consistently smaller than our data. However, the increasing difference, reaching 7.6 units at $c = 4$ mol dm^{-3}, certainly arises from fitting a Debye equation to the few of frequencies

investigated in that study. This probably also accounts for the discrepancies in τ. In 1971, Strogyn fitted the available literature data of $\epsilon(c,\vartheta)$ and $\tau(c,\vartheta)$.[37] At his highest concentration, $c = 3$ mol dm^{-3}, the permittivity calculated from his equations is considerably smaller than the present results at all temperatures, reaching a deviation of 24% at 35 °C. On the other hand, τ is 22% smaller at 5 °C, comparable around room temperature, and 10% larger at 35 °C. Again, the limited number of frequencies covered in Strogyn's sources offers a possible explanation. More problematic are the discrepancies with the data of Pottel et al., who investigated the pressure dependence of $\hat{\epsilon}(\nu)$ in the range $1 \le \nu(\mathrm{GHz}) \le 25$[39] for a 5 mol dm^{-3} NaCl solution. At 25 °C they obtained $\epsilon = 38.7$ and $\tau = 5.5$ ps, i.e., values that are approximately 8% and 15% smaller than our extrapolated data, although they found a comparable Cole−Cole parameter. On the other hand, at 5 °C, ϵ and α are comparable with our data but again τ is 20% smaller.

One reason for the deviations of the static permittivity is a systematic error of the VNA. Measurements with water, dimethylformamide, methanol, and dimethylsulfoxide as the standard liquids (of permittivity ϵ_{cal} taken from ref 9) in the calibration sequence air/mercury/standard liquid, performed with samples (various organic liquids and ethanol−water mixtures) covering the permittivity range $19.4 \le \epsilon \le 78.4$ revealed a deviation, $\Delta_{VNA} = \epsilon - \epsilon_{VNA}$, between the accepted permittivity values, ϵ, and the VNA result, ϵ_{VNA}, given by the expression $\Delta_{VNA} = (0.021 \pm 0.002)(\epsilon - \epsilon_{cal})$. However, it should be noted that $\Delta_{VNA} \le 0.95$ for the investigated NaCl solutions, which is comparable to the scatter of ϵ at high concentrations (Tables 3S−6S of the Supporting Information). As the application of the above result to conducting samples is not straightforward, we have abstained from correcting $\epsilon(c)$. Although the reliability of the reference data is limited and even though our data of $\epsilon(c,\vartheta)$ and $\tau(c,\vartheta)$ exhibit a smooth change with temperature and concentration, which can be interpreted in a self-consistent way (Section 4), it is clear from the above discussion that at present a satisfactory assessment of the accuracy of $\hat{\epsilon}(\nu)$ is not possible at $c > 1$ mol dm^{-3}. Since DRS studies of technically relevant concentrated electrolyte solutions are of increasing interest and since adequate instrumentation is now commercially available, the accurate determination of reference systems involving different experimental techniques and laboratories seems highly desirable.

4. Discussion

4.1. Solvent Dispersion Amplitude. The marked decrease of the solvent permittivity, $\epsilon(c)$, or more exactly of the solvent dispersion amplitude (relaxation strength), $S(c) = \epsilon(c) - \epsilon_\infty(c)$, with increasing electrolyte concentration, c, is currently thought to arise from two additive contributions[4,6]

$$\Delta\epsilon(c) = S(0) - S(c) = \Delta_{eq}\epsilon(c) + \Delta_{kd}\epsilon(c) \qquad (10)$$

The equilibrium term $\Delta_{eq}\epsilon(c)$ comprises the dilution of the solvent dipole density by the nonpolar ions ($\epsilon_{ion} \approx 2$) and the connected change of the internal field. In addition, the strong ion−solvent interactions induce a partial "freezing" (irrotational bonding, IB) of solvent molecules in the vicinity of the ions, which leads to a cancellation of dipole moments in the ionic solvation shells. Hence, a comparison of the apparent water concentration in the solution, c_s^{ap}, calculated from $S(c)$, with the analytical solvent concentration, c_s, allows the determination of the effective solvation number.

$$Z_{IB}(c) = (c_s - c_s^{ap})/c \qquad (11)$$

Z_{IB} is the average number of water molecules per equivalent of electrolyte that are (at a given time) unable to contribute to the solvent relaxation process. But note that generally the residence time of a water molecule in the hydration shell of an ion is on the order of pico- to nanoseconds.

The kinetic depolarization (kd) term in eq 10, $\Delta_{kd}\epsilon(c)$, arises from the relative motion of the ions and the surrounding solvent molecules in the external field. According to the continuum theory of Hubbard et al.,[40,41] kd is proportional to the solution conductivity, κ, with the slope ξ determined by the dielectric properties of the pure solvent. For a solvent with Debye-type relaxation behavior, kinetic depolarization is given by

$$\Delta_{kd}\epsilon(c) = \xi\kappa(c); \quad \xi = p\frac{\epsilon(0) - \epsilon_\infty(c)}{\epsilon(0)}\frac{\tau(0)}{\epsilon_o} \qquad (12)$$

The factor p accounts for the hydrodynamic boundary conditions of *stick* ($p = 1$) or *slip* ($p = 2/3$) ionic motion.

Several approaches, reviewed in refs 4 and 5 have been suggested for the calculation of c_s^{ap} from the equilibrium amplitude of the solvent dispersion

$$S_{eq}(c) = S(c) + \Delta_{kd}\epsilon(c) \qquad (13)$$

As shown in the comparative discussion of ref 30, the results obtained for a given electrolyte are model dependent and no particular model is yet favored so that a direct comparison of Z_{IB} data from different sources is not straightforward. Moreover, some of the models are strictly valid only at $c \to 0$.

To compare our data with those of refs 12 and 30, which were obtained using a variant of Lestrade's model,[42] our analysis also starts from the Kirkwood−Froehlich (KF) equation[22]

$$\frac{(\epsilon - \epsilon_\infty)(2\epsilon + \epsilon_\infty)}{\epsilon(\epsilon_\infty + 2)^2} = \frac{N_A g\mu^2}{9k_B T\epsilon_o}c_s \qquad (14)$$

where k_B is the Boltzmann constant, μ is the gas-phase dipole moment of water, and g is the Kirkwood correlation factor. By normalizing to the data of pure water, $c = 0$, to minimize ambiguities in the choice of the infinite frequency permittivity and in the treatment of the cavity and reaction fields,[28] the apparent solvent concentration is obtained as

$$c_s^{ap}(c) = \frac{g(c)}{g(0)}c_s^{bulk} = c_s(0)F_{KF}\frac{2\epsilon(c) + \epsilon_\infty(0)}{\epsilon(c)}S_{eq}(c) \qquad (15)$$

with

$$F_{KF} = \frac{\epsilon(0)}{(\epsilon(0) - \epsilon_\infty(0))(2\epsilon(0) + \epsilon_\infty(0))} \qquad (16)$$

Note that the infinite frequency permittivity is fixed at $\epsilon_\infty(0)$ in our data analysis and that only the product $g(c)c_s^{bulk}(c)$ is accessible from eqs 14 and 15 instead of the concentration of undisturbed bulk water, $c_s^{bulk}(c)$.

With $\epsilon(c)$ calculated from the parameters of Table 1, the effective solvation numbers $Z_{IB}(c)$ are obtained for NaCl (Figure 5). Included in the diagram are the results for negligible kinetic depolarization, $\xi = 0$, and for eq 12 with *slip* boundary conditions. $\xi = \xi_{stick}$ yields unrealistic values of $Z_{IB}(c) \le 0$. Whereas the data for $\xi = 0$ are constant at low concentration, reflecting the linear decrease of $\epsilon(c)$ in this range (except for

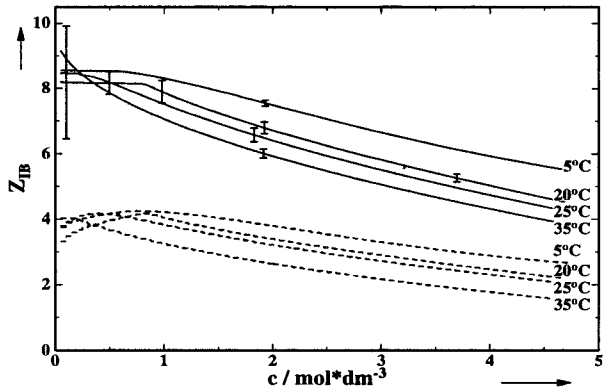

Figure 5. Effective solvation number, Z_{IB}, of NaCl in water as a function of electrolyte concentration and temperature. Broken lines are under the assumption of kinetic depolarization (eq 12) with *slip* boundary conditions, solid lines are without kinetic depolarization, $\xi = 0$. The error bars, determined from $\sigma_{fit}(\epsilon)$ of Table 1, have the same magnitude for both sets of curves.

35 °C), the slight increase observed for the ξ_{slip} is due to the nonlinear variation of $\kappa(c)$. However, at $c < 1$ mol dm^{-3}, these changes are within the error limits of the data (essentially determined by $\sigma_{fit}(\epsilon)/c$), as is the dependence of Z_{IB} on temperature over the range investigated ($5 \leq \vartheta(°C) \leq 35$). From the limit of Z_{IB} at $c \rightarrow 0$, approximated by

$$\lim_{c \rightarrow 0} Z_{IB} \approx a_1 + 2c_s(0)F_{KF}\delta_\epsilon \qquad (17)$$

where

$$a_1 = \lim_{c \rightarrow 0} \frac{dc_s(c)}{dc} = M_s^{-1} \lim_{c \rightarrow 0}\left[\frac{d\rho}{dc} - M_e\right] \qquad (18)$$

with ρ as the solution density, and M_s and M_e as the molar masses of solvent and electrolyte, respectively, the limiting effective solvation number of $Z_{IB}^{\xi=0} = 8.6 \pm 0.2$ is obtained for NaCl if kinetic depolarization is negligible (giving 1/7 relative weight to the 35 °C value compared to 2/7 for the other data). $Z_{IB}^{slip}(0) = 4.2 \pm 0.3$ is obtained if eq 12 with $p = 2/3$ is valid.

At $c \geq 1$ mol dm^{-3}, the errors become small enough to reveal a significant decrease of the effective solvation number with increasing electrolyte concentration both for $\xi = 0$ and $\xi = \xi_{slip}$. Also, Z_{IB} decreases with rising temperature, which indicates (as expected) that the competition of ion−solvent interactions and thermal motion determines the degree of IB for a given solvent at specified c.

Z_{IB} is an effective solvation number that may be taken as a measure of the relative strength of ion−solvent and solvent−solvent interactions at a given temperature. Usually Z_{IB} is different from the first-shell coordination number determined by scattering techniques or MD simulation because gc_s^{bulk} explicitly incorporates effects of the ionic fields on the bulk structure. It should be noted that for a solvent with $g(0) > 1$, like water, the expected breakdown of the bulk solvent structure with increasing concentration, i.e., a decrease of $g(c)$, should lead to an increase of Z_{IB} if the first solvation shell remains unchanged. Hence, a decreasing value of $Z_{IB}(c)$ with increasing c reflects a release of bound solvent molecules in the sense that the mobility of the water molecules in the solvation shell increases and their residence time decreases. Steric crowding and the decreasing number ratio of solvent molecules per ion offer an obvious explanation; in aqueous NaCl, a minimum distance of $d_{+-}^{min} = r_+ + r_- + 4r_s = 849$ pm, ($d_{++}^{min} = 776$ pm, $d_{--}^{min} = 932$ pm) is required for undisturbed first hydration shells (thickness $2r_s = 285$ pm[44]) of the ions (radii $r_+ = 98$ pm, $r_- = 181$ pm[43]). However, the average interionic distance in these solutions decreases from $\bar{d}_{ij} = 1180$ pm at $c = 0.5$ mol dm^{-3} to 940 pm at 1 mol dm^{-3} to 750 pm at 4 mol dm^{-3}, with $\bar{d}_{ij} = d_{+-}^{min}$ at 2.7 mol dm^{-3}. Additionally, the water-to-ion ratio of approximately 27:1 at $c = 1$ mol dm^{-3} drops to 16:1 at 4 mol dm^{-3}.

According to the data compiled by Ohtaki and Radnai,[45] diffraction studies and computer simulations give average coordination numbers (i.e., the number of water molecules in the first hydration shell) for Na^+ ranging from 4 to 8, with growing evidence for $\bar{n}_+ \approx 6$.[46−49] The dipole moments of these water molecules prefer a radial orientation within a narrow angular distribution. Cl^- has an average coordination number of $\bar{n}_- = 6$ with a broad distribution ranging from 1 to 8 (or even 13).[45,48−51] Although a large distribution of Cl···H−O angles is found, linear Cl^-−water hydrogen bonds predominate. The sparse data on the hydration-shell dynamics of both ions suggest that the reorientation of H_2O around the cation is slowed compared to bulk water, essentially being reduced to rotation around the axis defined by the dipole vector, whereas the water mobility around the anion is slightly increased. Note, however, that even for the anion, the rotation time of the solvent dipole moment in its first hydration shell is reduced.[52] The residence times of water molecules in the solvation shell of Cl^- and in the bulk are comparable but larger around the cation. For instance, Impey et al. give $\tau_{res}(H_2O) \approx \tau_{res}(Cl^-) \approx 4.5$ ps and $\tau_{res}(Na^+) \approx 9.9$ ps.[54] However, data from different sources show considerable scatter.[45−47,49,50,53] In summary, the above data suggest a labile anionic solvation shell with, at most, limited compensation of dipole moments but a highly symmetric and rather stable arrangement of water molecules around Na^+. It is therefore plausible to assign the effective solvation number determined with DRS entirely to the cation, $Z_{IB}(NaCl) = Z_{IB}(Na^+)$.

We may now compare these limiting effective cation solvation numbers, $Z_{IB}^{\xi=0}(Na^+,0) = 8.6 \pm 0.2$ and $Z_{IB}^{slip}(Na^+,0) = 4.2 \pm 0.3$, with available literature data. Obviously, this is complicated by the availability of two markedly different DRS results. However, $Z_{IB}^{\xi=0}$ cannot simply be rejected because recent computer simulations of Chandra and Patey suggest $\xi = 0$ for moderate to high electrolyte concentrations.[55] Also, the application of eq 12 is problematic. The equation is derived for a vanishing ionic radius at infinite dilution and does not take into account the observed dependence of $\Delta\epsilon(c)$, eq 10, on r_i ($i = +, -$), see Figure 3 of ref 23 and the accompanying discussion. The molecular model of ref 41 tackles this problem. However, the large normalized dielectric decrement predicted by this theory for Na^+ (see their Figure 2 for the data) results in a depolarization factor of $\xi \approx 0.9\xi_{stick}$, which gives $Z_{IB}(c) \leq 0$ at higher concentrations. On the other hand, the depolarization factor predicted by the molecular theory for large ions approaches ξ_{slip}. Since Na^+ has a well defined solvation shell by all accounts, it seems likely that the magnitude of the depolarization factor is determined by $r_+ + 2r_s$ and not the bare cation radius. Thus $\xi \approx \xi_{slip}$. On the basis of considerations of residence time and the self-diffusion coefficient, Kaatze draws the same conclusion for Li^+.[4] Additional support comes from the large effective Na^+ radius found by Balbuena et al. in their simulation study of ion transport in aqueous solution[52] and from the Stokes radius, $r_{St}(Na^+) = 181$ pm, deduced from conductivity data.[56] It is important to emphasize that our $Z_{IB}(0)$ data cannot be

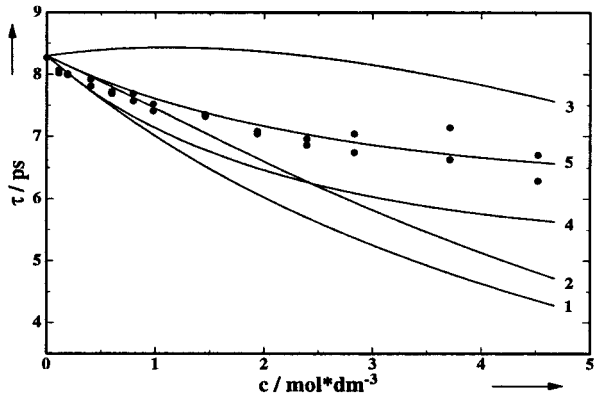

Figure 6. Experimental water relaxation times, τ, at 25 °C (symbols) and calculated values according to the rate constant model, eq 21 (lines). Parameters are as follows: (curves 1−4) $\tau_+ = 20$ ps, $\tau_- = 3$ ps, $\tau(0) = 8.3$ ps; (curve 1) $n_+ = n_- = Z_{IB}{}^{\xi=0}(0) = 8.6$; (curve 2) $n_+ = Z_{IB}{}^{\xi=0}(c)$, $n_- = 6$, (curve 3) $n_+ = Z_{IB}{}^{\xi=0}(c)$, $n_- = 2$, (curve 4) $n_+ = n_- = Z_{IB}{}^{\xi=0}(c)$, (curve 5) $\tau_+ = 20$ ps, $\tau_- = 3.7$ ps, $\tau(0) = 8.3$ ps, and $n_+ = n_- = Z_{IB}{}^{\xi=0}(c)$.

directly compared with the Z values of ref 23 due to different starting assumptions. However, the comparable δ_ϵ (Section 3) results in a similar $Z_{IB}(0)$ value.

The average coordination number from scattering experiments and computer simulations, $\bar{n}_+ \approx 6$, lies between the $\xi = 0$ and the $\xi = \xi_{slip}$ limits of $Z_{IB}(Na^+,0)$. Arguments can be made to reconcile either effective solvation number with $\bar{n}_+$ but obviously a direct comparison of Z_{IB} with the coordination number is not possible. The primary solvation number, n_{PSO}, defined Bockris and Reddy[57] as the number of solvent molecules that lose their independent translational freedom and move with the ion, seems more appropriate. Indeed, $Z_{IB}{}^{slip}(Na^+,0) = 4.2 \pm 0.3$ compares favorably with their value of $n_{PSO}(Na^+) = 4 \pm 1$. Marcus deduces $n_{PSO}(Na^+) = 3.9$ from apparent molal isothermal compressibilities but smaller values of activity coefficients and hydration entropies.[58] On the other hand, Bockris and Reddy as well as Marcus give $n_{PSO}(Cl^-) = 2 \pm 1$ as the most probable value for the chloride ion, which seems incompatible with our definition $Z_{IB}{}^{slip}(Cl^-,0) = 0$. However, the hydration entropy result dominates this average value of the primary solvation number. Compressibility and apparent molal volume also suggest negligible anion hydration.

Barthel et al. also assumed $Z_{IB}{}^{slip}(Cl^-,0) = 0$ and found a self-consistent series of ionic $Z_{IB}(0)$ data for a series of 1:2, 2:1, and 2:2 electrolytes, when kinetic depolarization under *slip* boundary conditions was assumed to apply. These data also correlate favorably with primary solvation numbers of Bockris and Reddy, whereas the assumptions $\xi = 0$ and $\xi = \xi_{stick}$ yield an inconsistent series of ionic $Z_{IB}(0)$.[30] From the sequence $Cl^- \rightarrow CdCl_2 \rightarrow CdSO_4 \rightarrow Na_2SO_4$ and $Cl^- \rightarrow MgCl_2 \rightarrow MgSO_4 \rightarrow Na_2SO_4$ Barthel et al. deduce the average value of $Z_{IB}{}^{slip}(Na^+,0) = 4.5$ which is in good agreement with our more direct result. Combining $Z_{IB}{}^{slip}(Na^+,0) = 4.2$ of this work with the data given for NaF and KF in ref 12, values for $Z_{IB}{}^{slip}(F^-,0) = 5.3$ and $Z_{IB}{}^{slip}(K^+,0) = 1.3$ can be determined, which are in reasonable agreement with the primary solvation numbers of these ions, $n_{PSO}(F^-) = 4 \pm 1$ and $n_{PSO}(K^+) = 3 \pm 2$.[57] In contrast, $\xi = 0$ would require $Z_{IB}{}^{\xi=0}(K^+,0) = 7.8$.

The above discussion strongly suggests that, for aqueous electrolyte solutions, the dielectric properties of the solvent exhibit kinetic depolarization with *slip* boundary conditions of ionic motion. This implies that the impact of the solvated ions on the structure of the bulk water is small. The apparent superiority of the continuum theory of kd[40,41] versus the molecular model[41] is understandable in the light that the latter approches the ξ_{slip} limit of eq 12 and that, within the limited data currently available, the small and highly charged ions bear effective solvation numbers Z_{IB} compatible with a well-defined first hydration shell. Dielectric data for 1:1 electrolytes in methanol are also compatible with *slip* kinetic depolarization,[59] although the data for 1:1 electrolytes in acetonitrile suggest $\xi = 0$.[60]

4.2. Solvent Relaxation Time. For pure water $\tau^{-1}(T)$ can be interpreted as a rate constant characterizing the formation of "mobile water"; that is, τ gives the dwelling time of a water molecule as it passes from the ground state determined by water's average number of hydrogen bonds to the activated state, where at most a single H-bond is left. Fast reorientation of this molecule into a new equilibrium position will generally lead to a major fluctuation of the macroscopic dipole moment $\vec{M}(t) = \sum_i \vec{\mu}_i$.[28] Following an approach similar to Giese's theory of weighted rotational correlation times[61] but stressing the "chemical" interpretation of τ, one may therefore assume that in the case of aqueous electrolyte solutions $\tau^{-1}(c)$ reflects the weighted average rate of this process for the subspecies *bulk* water (relaxation time $\tau(0)$ of the pure solvent, fraction $x_{bulk} = 1 - x_+ - x_-$ of the analytical concentraton of water), water in the solvation shell of the cation (τ_+, x_+) and of the anion (τ_-, x_-), according to

$$\tau^{-1}(c) = x_+\tau_+{}^{-1} + x_-\tau_-{}^{-1} + (1 - x_+ - x_-)\tau^{-1}(0) \quad (19)$$

Equation 19 requires that the envelope of the three superimposed contributions of comparable relaxation times, which defines the experimental spectrum, is suffiently close to the Cole−Cole distribution obtained in the fitting procedure. It seems plausible that the upper limits of τ_+ and τ_- should be given by residence times of the water molecules in the solvation shells of the cation and the anion. According to Ohtaki and Radnai,[45] the residence time of water in the first solvation shell of Cl^- is around 4 ps and "long" for Na^+. One may therefore assume $\tau_- < \tau(0) < \tau_+$. Although distributed over a large angle, the orientation of water around the anion is dominated by linear HO−H···Cl^- hydrogen bonds. So, even if the strength of this bond exceeds that of the H-bond between water molecules, as is sugested by the MD simulation results of Flanagin et al.,[53] implying $\tau_- > \tau(0)$, rotation around O−H···Cl^- after breakage of the H-bonds between solvation shell water and the bulk is dielectrically active. In contrast, the dipole moments of the water molecules in the first solvation shell of Na^+ are oriented radially and have a much smaller angular distribution. This leads to a net cancellation of moments that pertains if the hydrogen bonds between the bulk and a molecule in the first hydration shell are broken. Hence, on average, Z_{IB} water molecules per cation will be inactive dielectrically but the release rate of those molecules will nevertheless be proportional to $Z_{IB}c$.

Figure 6 shows that eq 19 yields a variety of curves that ressemble experimental water relaxation times in electrolyte solutions (see Figure 5 of ref 30), especially if concentration-dependent solvation numbers are allowed. The problem is then to find reasonable "guesses" for the parameters. From the above arguments, we may identify $Z_{IB}(Na^+,0)$ with the effective solvation number of Na^+, suggesting for the fractions $x_+ = (Z_{IB}c)/c_s$ and $x_- = (n_-c)c_s$; $n_-(c)$ is the a priori concentration-dependent solvation number of the anion. Expressed in terms of the apparent water concentration, $c_s{}^{ap}$, obtained from the water dispersion amplitude, this is

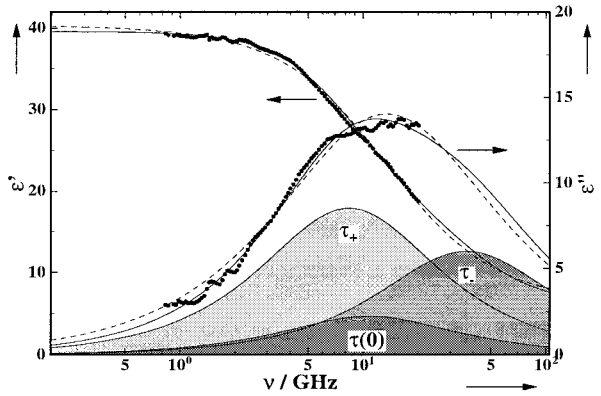

Figure 7. Experimental dielectric dispersion, $\epsilon'(\nu)$, and loss data, $\epsilon''(\nu)$, of a 4.643 mol dm^{-3} NaCl solution in water at 5 °C (symbols) and the spectrum predicted by the three-state model for $\tau(c)$ (solid line). Also indicated are the predicted loss contributions of the free water ($\tau(0)$) and of the water surrounding the cations (τ_+) and the anions (τ_-). The broken line represents the Cole−Cole fit to $\hat{\epsilon}(\nu)$.

$$\tau^{-1}(c) = \frac{c_s - c_s^{ap}}{c_s}[\tau_+^{-1} - \tau^{-1}(0)] + \frac{n_-(c)c}{c_s}[\tau_-^{-1} - \tau^{-1}(0)] + \tau^{-1}(0) \quad (20)$$

Curves 2 ($n_- = 6$) and 3 ($n_- = 2$) of Figure 6 show that a constant anion solvation number is not compatible with the experimental data, whereas the unlikely assumption $n_- = Z_{IB}$ produces the right curvature (curves 4 and 5).

If our interpretation that the decrease of $n_+ = Z_{IB}(Na^+, c)$ is caused by an increasing competition of all ions for the decreasing number of solvent molecules is correct, it seems reasonable to assume a similar decrease of $n_-(c)$ and identify $n_-(0) = \bar{n}_-$. Equation 20 may then be written as

$$\tau^{-1}(c) = \frac{c_s - c_s^{ap}}{c_s}\left[\tau_+^{-1} + \frac{\bar{n}_-}{Z_{IB}(Na^+,0)}\tau_-^{-1} - \tau^{-1}(0)\left(1 + \frac{\bar{n}_-}{Z_{IB}(Na^+,0)}\right)\right] + \tau^{-1}(0) \quad (21)$$

which allows the determination of the sum $k = (\tau^{-1} + \bar{n}_-\tau_-^{-1}/Z_{IB}(0))$ from the experimental data. The results, obtained with $\tau(0)$ preset to the specified value, are summarized in Table 2 for $\xi = 0$ and $\xi = \xi_{slip}$. As can be seen from Figure 3, eq 21 yields a good description of $\tau(c)$ at all investigated temperatures. Both sets of k exhibit similar values of the Arrhenius activation energy, $E_a(\xi{=}0) = 22 \pm 1$ kJ mol and $E_a(\xi_{slip}) = 22.7 \pm 0.3$ kJ mol, which are close to $E_a(\tau)$ at $c = 0.8$ mol dm^{-3}. Therefore, the value of k and/or the quality of the fit do not yield independent information on the magnitude of kinetic depolarization.

The structure of eq 21 permits the determination k from the experimental data, but does not provide a means to split it into its ionic contributions τ_+ and τ_-. Unfortunately, it is also impossible to introduce a simplifying assumption comparable to $Z_{IB}(Cl^-,0) = 0$ (which would enable such a splitting when more data become available in future). Solvation-shell residence times may define the possible limits of τ_+ and τ_-, but such data are rare and they give a rough estimate at best. The increase of the Cole−Cole distribution parameter at $c > 2$ mol dm^{-3} as well as the observation that the spectra of the concentrated solutions at 5 °C are better fitted by a superposition of two Debye processes provide a hint at the proposed three-state model. It is indeed possible to model, e.g., the spectrum of the 4.64 mol dm^{-3} solution at 5 °C, with parameters derived from an assumed value of $\tau_-(25\ °C) = 3.9$ ps (plausible as a lower limit from available residence times[45,54]), $E_a(k)$ and k at 25 and 5 °C; see Figure 7 for $\xi = 0$. However, more information is necessary to show whether the three-state model of eq 19 is a valid approach for the understanding of the solvent relaxation times of aqueous electrolyte solutions. Figure 7 suggests that at high concentrations $\hat{\epsilon}(\nu)$ should deviate significantly enough from a Cole−Cole distribution to extract $\tau(0)$, τ_+, and τ_- directly from the experimental spectra, provided a sufficiently large frequency range (preferably $0.5 \le \nu$ (GHz) ≤ 100) is covered with at least twice our accuracy.

5. Conclusions

The present work shows that commercial VNA systems are able to measure complex permittivity spectra of electrolyte solutions up to unusually high concentrations and conductivities over quite a large range of frequencies with a precision and accuracy similar to that obtained by TDS and waveguide systems provided a judicious calibration procedure is followed. Given the simplicity of the VNA system, which lends itself to facile extension to nonambient temperatures, such systems appear to be a very attractive alternative for DRS measurements. However, this work also reveals the urgent need of a joint effort by different laboratories combining the various techniques of DRSto define reliable complex permittivity standards for concentrated electrolyte solutions.

Data obtained in the present study show that at $c < 1$ mol dm^{-3} the effective solvation number of Na^+ is constant and (within the limits of error) independent of temperature, whereas at higher concentration, Z_{IB} decreases significantly. It is also shown that kinetic depolarization under *slip* boundary conditions of ionic motion is relevant for the dielectric properties of aqueous NaCl. A three-state model has been proposed to describe the dielectric relaxation time of aqueous electrolyte solutions. The model is able to fit $\tau(c,\vartheta)$ but requires independent confirmation. This could be done by determining the precise band shape of the complex permittivity spectra of concentrated

TABLE 2: Relaxation Time of Pure Water, $\tau(0)$, Average Coordination Number of the Anion, $\bar{n}_-$ (Ref 45), Limiting Number of Water Molecules Irrotationally Bound to Na^+, $Z_{IB}(Na^+,0)$, and Rate Constants $k = (\tau_+^{-1} + n_-\tau_-^{-1}/Z_{IB}(Na^+,0))$ of Eq 21 of Aqueous NaCl Solutions as a Function of Temperature, ϑ

			$\xi = 0$		$\xi = \xi_{slip}$	
ϑ	$\tau(0)$	$\bar{n}_-$	$Z_{IB}^{\xi=0}(Na^+,0)$	k	$Z_{IB}^{slip}(Na^+,0)$	k
5	15.50			0.146 ± 0.001		0.235 ± 0.002
20	9.43			0.247 ± 0.002		0.394 ± 0.004
		6	8.6 ± 0.2		4.2 ± 0.3	
25	8.15			0.287 ± 0.002		0.463 ± 0.004
35	6.34			0.366 ± 0.004		0.62 ± 0.01

[a] Units: ϑ in °C, $\tau(0)$ in 10^{-12} s, k in 10^{12} s^{-1}. [b] Data are given for negligible kinetic depolarization, $\xi = 0$, and for kinetic depolarization under *slip* conditions, $\xi = \xi_{slip}$.

electrolytes with improved accuracy over a larger frequency range than is currently possible in our laboratory.

Acknowledgment. This work was funded by the Australian alumina industry through the Australian Mineral Industries Research association Project P380B. Support by the Deutsche Forschungsgemeinschaft for R.B. is gratefully acknowledged. The authors thank Prof. J. Barthel and Dipl. Chem. C. Baar for providing the ELDAR results and Prof. E. Guàrdia for helpful discussions on solvation shell dynamics.

Supporting Information Available: Tables of the dielectric relaxation parameters, interpolated densities and conductances of the investigated NaCl solutions. This information is available free of charge via the Internet at http://pubs.acs.org.

References and Notes

(1) Farber, H.; Petrucci, S. Dielectric Spectroscopy. In *The Chemical Physics of Solvation*; Dogonadze, R. R., Kálmán, E., Kornyshev, A. A., Ulstrup, J., Eds.; Elsevier: Amsterdam, 1986; Part B.
(2) Ohmine, I.; Tanaka, H. *Chem. Rev.* **1993**, *93*, 2545.
(3) Kaatze, U. *Radiat. Phys. Chem.* **1995**, *45*, 549.
(4) Kaatze, U. *J. Solution Chem.* **1997**, *26*, 1049.
(5) Buchner, R.; Barthel, J. *Annu. Rep. Prog. Chem., Sect. C* **1994**, *91*, 71.
(6) Barthel, J.; Buchner, R.; Eberspächer, P.-N.; Münsterer, M.; Stauber, J.; Wurm, B. *J. Mol. Liq.* **1998**, *78*, 82.
(7) Zwanzig, R. *J. Chem. Phys.* **1970**, *52*, 3625.
(8) Falkenhagen, H. *Theorie der Elektrolyte*; Hirzel: Leipzig, 1971.
(9) Barthel, J.; Gores, H.-J. Solution Chemistry: A Cutting Edge in Modern Electrochemical Technology. In *Chemistry of Nonaqueous Solutions—Current Progress*; Mamantov, G., Popov, A. J., Eds.; VCH: New York, 1994.
(10) (a) Fawcett, W. R.; Tikanen, A. C. *J. Phys. Chem.* **1996**, *100*, 4251. (b) Tikanen, A. C.; Fawcett, W. R. *Ber. Bunsen-Ges. Phys. Chem.* **1996**, *100*, 634. (c) Fawcett, W. R.; Tikanen, A. C. *J. Mol. Liq.* **1997**, *73/74*, 373.
(11) Barthel, J.; Hetzenauer, H.; Buchner, R. *Ber. Bunsen-Ges. Phys. Chem.* **1992**, *96*, 1424.
(12) Buchner, R.; Hefter, G. T.; Barthel, J. *J. Chem. Soc., Faraday Trans.* **1994**, *90*, 2475.
(13) Whitfield, M. Seawater as an Electrolyte Solution. In *Chemical Oceanography*; Riley, J. P., Skirrow, G., Eds.; Wiley: London, 1975; Vol. 1.
(14) Johnson, K. S.; Pytkowicz, R. M. Ion Association and Activity Coefficients in Multicomponent Solutions. In *Activity Coefficients in Electrolyte Solutions*; Pytkowicz, R. M., Ed.; CRC Press: Boca Raton, 1979; Vol. 2.
(15) (a) Sipos, P.; Bodi, I.; May, P. M.; Hefter, G. Formation of $NaOH^{\circ}$ (aq) and $NaAl(OH)_4^{\circ}$ (aq) Ion-pairs in Concentrated Alkaline Aluminate Solutions. In *Progress in Coordination and Organometallic Chemistry*; Ondrejovicz, G., Sirota, A., Eds.; Slovak Technical Press: Bratislava, 1997. (b) Sipos, P.; Hefter, G.; May, P. M. *Aust. J. Chem.* **1998**, *51*, 445. (c) Sipos, P.; Capewell, S. G.; May, P. M.; Hefter, G.; Laurenczy, G.; Lukacs, F.; Roulet, R. *J. Chem. Soc., Dalton Trans.* **1998**, 3007. (d) Radnai, T.; May, P. M.; Hefter, G.; Sipos, P. *J. Phys. Chem. B* **1998**, *102*, 7841.
(16) (a) Mingos, D. M. P. *Res. Chem. Intermed.* **1994**, *20*, 85. (b) Gabriel, C.; Gabriel, S.; Grant, E. H.; Halstead, B. S. J.; Mingos, D. M. P. *Chem. Soc. Rev.* **1998**, *27*, 213.
(17) Galema, S. A. *Chem. Soc. Rev.* **1997**, *26*, 233.
(18) Nyfors, E.; Vainikainen, P. *Industrial Microwave Sensors*; Artech House: Norwood, 1989.
(19) Krazewski, A., Ed. *Microwave Aquametry, Electromagnetic Wave Interaction with Water-Containing Materials*; IEEE Press: New York, 1996.
(20) Hilland, J. *Meas. Sci. Technol.* **1997**, *8*, 901.
(21) Barthel, J.; Buchner, R.; Münsterer, M. ELECTROLYTE DATA COLLECTION, Part 2: Dielectric Properties of Water and Aqueous Electrolyte Solutions. In *Chemistry Data Series*; Kreysa, G., Ed.; DECHEMA: Frankfurt, 1995; Vol. XII.
(22) (a) Böttcher, C. F. J. *Theory of Electric Polarization*, 2nd ed.; Elsevier: Amsterdam, 1973; Vol. 1. (b) Böttcher, C. F. J.; Bordewijk, P. *Theory of Electric Polarization*, 2nd ed.; Elsevier: Amsterdam, 1978; Vol. 2.
(23) Nörtemann, K.; Hilland, J.; Kaatze, U. *J. Phys. Chem. A* **1997**, *101*, 6864.
(24) Göttmann, O.; Kaatze, U.; Petong, P. *Meas. Sci. Technol.* **1996**, *7*, 525.
(25) Ellison, W. J.; Lamkaouchi, K.; Moreau, J.-M. *J. Mol. Liq.* **1996**, *68*, 171.
(26) ELectrolyte DAta Regensburg is a subset of the database DETHERM (distributor: STN, Karlsruhe, Germany).
(27) (a) Rønne, C.; Thrane, L.; Åstrand, P.-O.; Wallqvist, A.; Mikkelsen, K. V.; Keiding, S. R. *J. Chem. Phys.* **1997**, *107*, 5319. (b) Keiding, S. R. Personal communication.
(28) Buchner, R.; Barthel, J.; Stauber, J. *Chem. Phys. Lett.*, in press.
(29) Barthel, J.; Buchner, R.; Hölzl, C. Unpublished results.
(30) Barthel, J.; Hetzenauer, H.; Buchner, R. *Ber. Bunsen-Ges. Phys. Chem.* **1992**, *96*, 988.
(31) Bevington, P. R. *Data Reduction and Error Analysis for the Physical Sciences*; McGraw-Hill: New York, 1969.
(32) Popp, K.-H. Dissertation, Regensburg, 1987; data tabulated in ref 21.
(33) Kaatze, U. *J. Phys. Chem.* **1987**, *91*, 3111.
(34) Giese, K.; Kaatze, U.; Pottel, R. *J. Phys. Chem.* **1970**, *74*, 3718.
(35) Hasted, J. B. *Aqueous Dielectrics*; Chapman and Hall: London, 1973.
(36) Zasetskii, A. Yu.; Lileev, A. S.; Lyashchenko, A. K. *Russ. J. Inorg. Chem.* **1994**, *39*, 990.
(37) Strogyn, A. *IEEE Trans. Microwave Theory Technol.* **1971**, *19*, 733.
(38) Barthel, J.; Schmithals, F.; Behret, H. *Z. Phys. Chem. NF* **1970**, *71*, 115.
(39) Pottel, R.; Asselborn, E.; Eck, R.; Tresp, V. *Ber. Bunsen-Ges. Phys. Chem.* **1989**, *93*, 676.
(40) (a) Hubbard, J. B.; Onsager, L. *J. Chem. Phys.* **1977**, *67*, 4850. (b) Hubbard, J. B. *J. Chem. Phys.* **1978**, *68*, 1649.
(41) Hubbard, J. B.; Colonomos, P.; Wolynes, P. G. *J. Chem. Phys.* **1979**, *71*, 2652.
(42) Lestrade, J.-C.; Badiali, J.-P.; Cachet, H. *Dielectr. Relat. Mol. Processes* **1973**, *2*, 106.
(43) Barthel, J.; Gores, H.-J.; Schmeer, G.; Wachter, R. *Top. Curr. Chem.* **1983**, *111*, 33.
(44) Gibbs, J. H.; Cohen, C.; Fleming, P. D., III.; Porosoff, H. *J. Solution Chem.* **1973**, *2*, 277.
(45) Ohtaki, H.; Radnai, T. *Chem. Rev.* **1993**, *93*, 1157.
(46) Guàrdia, E.; Padró, J. A. *J. Phys. Chem.* **1990**, *94*, 6049.
(47) Smith, D. E.; Dang, L. X. *J. Chem. Phys.* **1994**, *100*, 3757.
(48) Balbuena, P. B.; Johnston, K. P.; Rossky, P. J. *J. Phys. Chem.* **1996**, *100*, 2706.
(49) Koneshan, S.; Rasaiah, J. C.; Lynden-Bell, R. M.; Lee, S. H. *J. Phys. Chem. B* **1998**, *102*, 4193.
(50) Guàrdia, E.; Padró, J. A. *Mol. Simul.* **1996**, *17*, 83.
(51) Powell, D. H.; Neilson, G. W.; Enderby, J. E. *J. Phys.: Condens. Matter* **1993**, *5*, 5723.
(52) Balbuena, P. B.; Johnston, K. P.; Rossky, P. J.; Hyun, J.-K. *J. Phys. Chem. B* **1998**, *102*, 3806.
(53) Flanagin, L. W.; Balbuena, P. B.; Johnston, K. P.; Rossky, P. J.; Hyun, J.-K. *J. Phys. Chem.* **1995**, *99*, 5196.
(54) Impey, R. W.; Madden, P. A.; McDonald, I. R. *J. Phys. Chem.* **1993**, *87*, 5071.
(55) Chandra, A.; Patey, G. N. *J. Chem. Phys.* **1994**, *100*, 8385.
(56) Oelkers, E. H.; Helgeson, H. C. *J. Solution Chem.* **1989**, *18*, 601.
(57) Bockris, J. O'M.; Reddy, A. K. N. *Modern Electrochemistry*, 3rd ed.; Plenum: New York, 1970; Vol. 1. It should be noted that the techniques considered by the authors as appropriate for the determination of n_{PSO} may yield considerably different results; see their Tables 2.19 and 2.20.
(58) Marcus, Y. *Ion Solvation*; Wiley: Chichester, 1985.
(59) Barthel, J.; Buchner, R.; Bachhuber, K.; Hetzenauer, H.; Kleebauer, M.; Ortmeier, H. *Pure Appl. Chem.* **1990**, *62*, 2287.
(60) Barthel, J.; Kleebauer, M.; Buchner, R. *J. Solution Chem.* **1995**, *24*, 1.
(61) Giese, K. *Ber. Bunsen-Ges. Phys. Chem.* **1972**, *76*, 495.